

# Compact Polarization Analysis Module for Optical Freespace Communication based on Dielectric Metasurface Gratings

Thomas Flügel-Paul<sup>(1)</sup> and Fabian Steinlechner<sup>(2)</sup>

<sup>(1)</sup>Fraunhofer Institute for Applied Optics and Precision Engineering,  
Albert-Einstein-Strasse 7, D-07745 Jena, Germany  
+49 6341 807434  
thomas.fluegel-paul@iof.fraunhofer.de

<sup>(2)</sup>Fraunhofer Institute for Applied Optics and Precision Engineering,  
Albert-Einstein-Strasse 7, D-07745 Jena, Germany  
+49 6341 807434  
fabian.steinlechner@iof.fraunhofer.de

## ABSTRACT

Quantum cryptography or quantum key distribution (QKD) provides encryption keys whose security can be ensured by the very laws of quantum physics. Unlike classical key distribution protocols, where the security is based on the presumed hardness of solving certain mathematical problems, encryption keys generated via QKD maintain their security irrespective of all future advance of computational power.

Utilizing the polarization of light is a simple and well-established technique for encoding a qubit – the most fundamental entity of information processing in optical communication. Here we propose an ultra-compact approach for the realization of a polarization analysis module utilizing dielectric optical metasurface gratings. The proposed optical configuration integrates frequency multiplexing and polarization state analysis functionality into a single component. In comparison with classical schemes and setups which address the same functionality, the here presented approach promises a considerable reduction in volume and mass and even complexity of the optical arrangement. In its most compact configuration, three flat optical elements are sequentially stacked in direct contact such that the overall element can be as thin as only a few millimeters.

## 1. INTRODUCTION

The interest in free-space and satellite-based QKD systems is continuously increasing over the last years. To minimize diffraction loss, these systems use beam sizes and apertures that are larger than those usually applied in classical communications. In free-space systems, the key generation is based in most cases on the polarization of single photons or entangled photon pairs, but a key challenge is to realize polarization analysis modules and multiplexers of suitable dimension.

Passive as well as active systems are known to perform polarization measurements. In passive systems an optical element, for example a beam splitter is used to split up the beam path and thus enable the measurement in two different bases by additional polarization elements, for example polarizer and detectors. The disadvantage of a passive system is the large number of optical components and the high losses in the system to measure in two mutually unbiased bases, as required by most QKD protocols [1,2].

In active systems the base in which to measure is determined by an active polarization influencing element, for example an electro optical modulator switching between the two bases to be measured followed by a polarization element, for example polarizer and detectors. The disadvantage of an active

system is the higher loss of the polarization influencing element and the necessity to use additional elements to enable a random base choice, as required by most QKD protocols.

Here we propose a new and compact approach for the realization of a polarization analysis module utilizing dielectric optical metasurfaces. The proposed optical configuration integrates frequency multiplexing and polarization state analysis functionality into a single component. The core component consists of only two functional optical meta-surface gratings, each of it implemented on a flat substrate with typical thickness in the order of only a millimeter. In its most compact configuration, 3 elements are sequentially stacked in direct contact such that the overall element is as thin as only a few millimeters. The lateral extension (and thus beam size) is arbitrary, however, in practice it will be restricted by available lithographic manufacturing technologies. Conveniently accessible lateral dimensions are diameters up to 150mm (6inch) and a scaling up to 300mm (12inch) seems within reach, which makes the devices ideally suited to applications in a long-distance free-space, and satellite-based QKD.

The contribution is structured as follows: In Section 2, we will provide a very brief introduction into the topic of meta-surfaces and so-called Berry-phase structures. The focus lies on its specific polarization response and suitable material systems for their realization. In Section 3, we will outline the classical problem of passive polarization state analysis together with typical “optical bench” configurations. In Section 4 we present a new and compact configuration relying on two specific Berry-phase metasurface gratings. In Section 5 we will provide details about the meta-structure itself, which is designed to work within the ITU grid, essentially between wavelengths from 1530nm to 1570nm. Finally, we will present modelled optical performance results.

## 2. BERRY PHASE METASURFACES

Metasurfaces are functional optical surfaces composed by purposefully designed nanostructures (called meta-structures) with typical extensions or feature size smaller than that of the wavelength of the interacting light. The fundamental approach is similar to that of classical diffractive optics, i.e., allowing to control amplitude and phase of the impinging beam at each location of the metasurface independently. However, the utilization of metasurfaces promises larger degrees of freedom in optical design and thus the element’s functionality. Metasurfaces allow higher control of chromatic dispersion and/or allow manipulating the state of polarization of light. Since the overall research on metasurfaces is overwhelming, we refer to some review articles which help to acquire an overview [3,4].

A special class of structures are so-called Pancharatnam-Berry meta-surfaces (often only called Berry phase elements). When a circularly polarized wave is incident, full phase control from 0 to  $2\pi$  of the cross-polarized output light that has the opposite handedness is possible by changing only the orientation of the unit structure [5,6]. By spatially arranging purposefully rotated copies of one and the same fundamental entity (the meta-atom), any continuous phase distribution can be realized [7]. The overall efficiency then depends only on the suitable design of the meta-atom.

For the sake of clarity and for better understanding of the following sections, we will recover the main characteristics of Berry phase elements.

**Basic layout of the metasurface.** The simplest but already very effective meta-atom which can be used for building up a functional meta-surface is a small elongated *pillar* of dielectric material. It is characterized by its three Cartesian extensions as depicted in Figure 1. Using lithographic manufacturing technologies (similar to semi-conductor processing) allows to populate large two-dimensional areas (e.g. on wafers or photo masks) where the orientation of each element can be flexibly controlled. *Figure 1* shows an SEM top view image of a manufactured pattern where the rotation angle increases in a linear fashion in one of the two lateral dimensions.

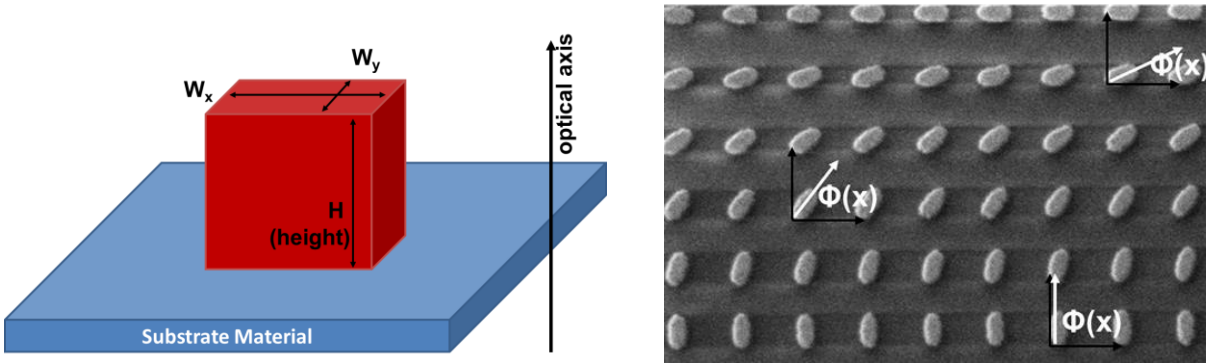


Figure 1. Left: Sketch of the three-dimensional layout of an elongated pillar of dielectric material with its characteristic dimensions labeled accordingly. Right: SEM top view image a Berry metasurface manufactured via electron beam lithography. The orientation of the long axis of the pillar is highlighted at some selected locations.

Finally, the optical function of such pattern is mainly governed by two contributions: First, the exact dimension of the pillar and its material (refractive index). Second, the local orientation of the pillars as encoded by rotation angle  $\phi(x,y)$  being a function of both lateral dimensions in general.

### Interaction with polarized light.

Berry phase elements can be designed for operation either in reflection or in transmission depending on whether the substrate material is reflective (e.g. metal) or transparent (e.g. glass). In the following we will restrict the discussion to transparent substrates. When a polarized collimated wave characterized by Jones vector  $|\mathbf{j}_{IN}\rangle$  is incident, the transmitted light field is composed of three different components.

- 1) Term A: a phase modulation function proportional to  $\exp(+2i * \phi(x,y))$   $|\mathbf{RHC}\rangle$
- 2) Term B: the complementary phase function proportional to  $\exp(-2i * \phi(x,y))$   $|\mathbf{LHC}\rangle$
- 3) Term C: a bias term with no phase modulation at all being proportional to  $|\mathbf{j}_{IN}\rangle$

$|\mathbf{RHC}\rangle$  and  $|\mathbf{LHC}\rangle$  denotes right-handed circular and left-handed circular polarized light.

The amount of light within each term depends on the polarization of the incident beam as well as the dimensions of the single pillar itself.

Two examples which are important for the following article are outlined in more detail. In the first case, the single pillar acts as a half-wave-retarder (HWR), i.e. introducing a phase shift of  $\pi$  between linearly polarized components directing along the axis of the pillar. In the second case, the single pillar acts as a quarter-wave-retarder (QWR). The following table provides the contribution of each abovementioned term for selected input polarizations  $|\mathbf{j}_{IN}\rangle$ .

Table 1. Theoretical limit of the decomposition of an incident polarized wave into three fundamental components after interaction with a Berry phase metasurface. The single meta-atom (pillar) is assumed to operate either as a perfect QWR (left table) or as a perfect HWR (right table).

QWR				HWR			
$\mathbf{j}_{IN}$	Term A	Term C	Term B	$\mathbf{j}_{IN}$	Term A	Term C	Term B
$ 0\rangle$	25%	50%	25%	$ 0\rangle$	50%	0%	50%
$ 90\rangle$	25%	50%	25%	$ 90\rangle$	50%	0%	50%

$ 45\rangle$	25%	50%	25%
$ 135\rangle$	25%	50%	25%
$ LHC\rangle$	50%	50%	0%
$ RHC\rangle$	0%	50%	50%

$ 45\rangle$	50%	0%	50%
$ 135\rangle$	50%	0%	50%
$ LHC\rangle$	100%	0%	0%
$ RHC\rangle$	0%	0%	100%

$|0\rangle$  and  $|90\rangle$  denotes horizontally and vertically linear polarized light.  $|45\rangle$  and  $|135\rangle$  denotes diagonally and anti-diagonally linear polarized light, respectively.

In conclusion, both Berry phase elements (composed of QWR or HWR meta-atoms) act as *polarization beam splitters* for circular polarized states, however, the QWR element still transmits 50% of the incident light without any changes (refer to Term C), whereas the HWR element does not.

**Typical Material Systems.** Reference [2] provides an overview of several choices of material systems covering reflective as well as transmissive metasurfaces. The main criterium for selection is the operational wavelength. In a nutshell, silicon on glas is the material system of choice for any infrared wavelength larger than  $\sim 900\text{nm}$ . On the other hand, titanium dioxide on glas is widely used in the visible spectrum down to  $\sim 400\text{nm}$  before the intrinsic absorption of titanium dioxide increases rapidly.

### 3. POLARIZATION STATE ANALYSIS – STATE OF THE ART

Most QKD protocols require the measurement of polarization of single photons in two mutually unbiased bases.

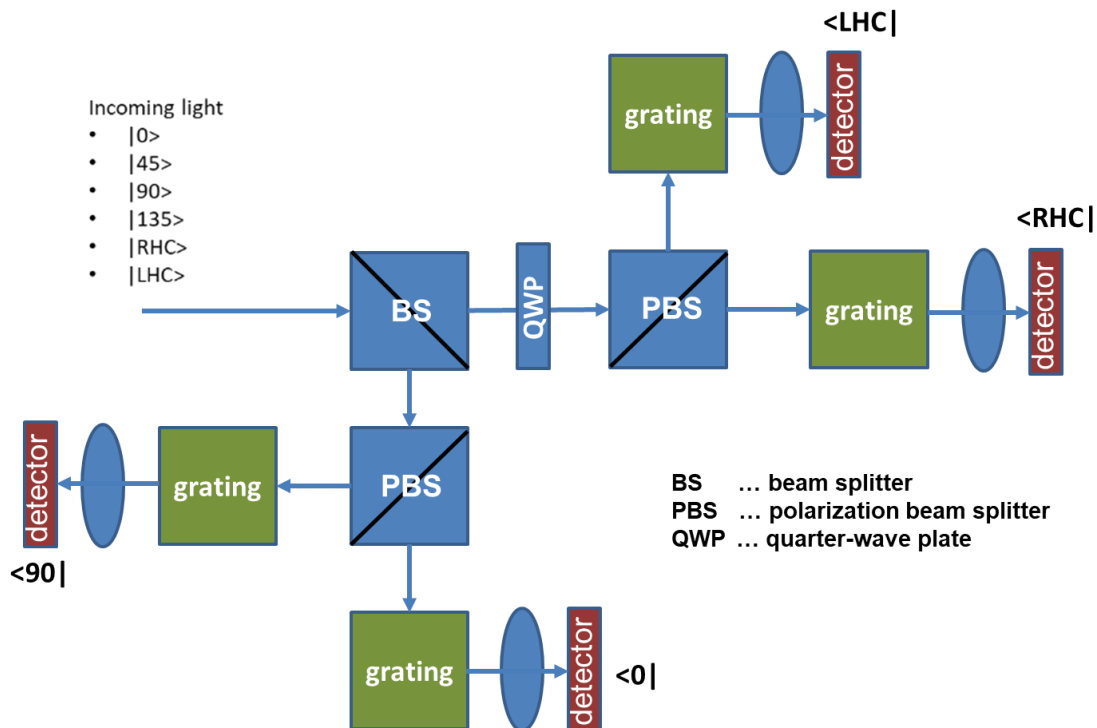


Figure 2. Classical scheme for polarization state analysis with decomposition into two mutually unbiased bases, i.e. linear and circular polarization.

Without loss of generality, we choose the following states:  $|0\rangle$ ,  $|90\rangle$ ,  $|LHC\rangle$  and  $|RHC\rangle$  and Figure 2 sketches the typical optical setup. With some minor modifications, any other choice or combination of polarization states might be adressable, too.

The most important components are the (unpolarized) beamsplitter (BS) and two polarization beam splitters (PBS) projecting the output onto purely linear polarized contributions. In practice, BS and PBS are typically optical cubes with specific coatings in between. Moreover, if the setup is aiming to work in multiple frequency channels simultaneously, then a set of dispersive elements (e.g. gratings) is needed to ensure the de-multiplexing into the individual signals.

In free-space QKD application, the typical extension of the above optics is in the order of the free-space communication beam size. The reason is, that any optics which does not preserve the state of polarization is not allowed to be used before the polarization beam splitting into the two unbiased bases is accomplished. Typical examples for optics which does not preserve the state of polarization are lenses or mirrors with high numerical aperture (e.g. for coupling the beam into a fibre or for focusing onto the detector) or diffraction gratings. In conclusion, any measure which helps to reduce the number of optical elements or, in general, the footprint of the above arrangement, will be desirable especially in satellite-based or airborne applications.

#### 4. NEW APPROACH TO POLARIZATION STATE ANALYSIS

An entirely new approach for a polarization state analysis scheme is depicted in Figure 3. The here introduced configuration achieves the same functionality as those outlined in Figure 2, however, the number of required elements is drastically reduced.

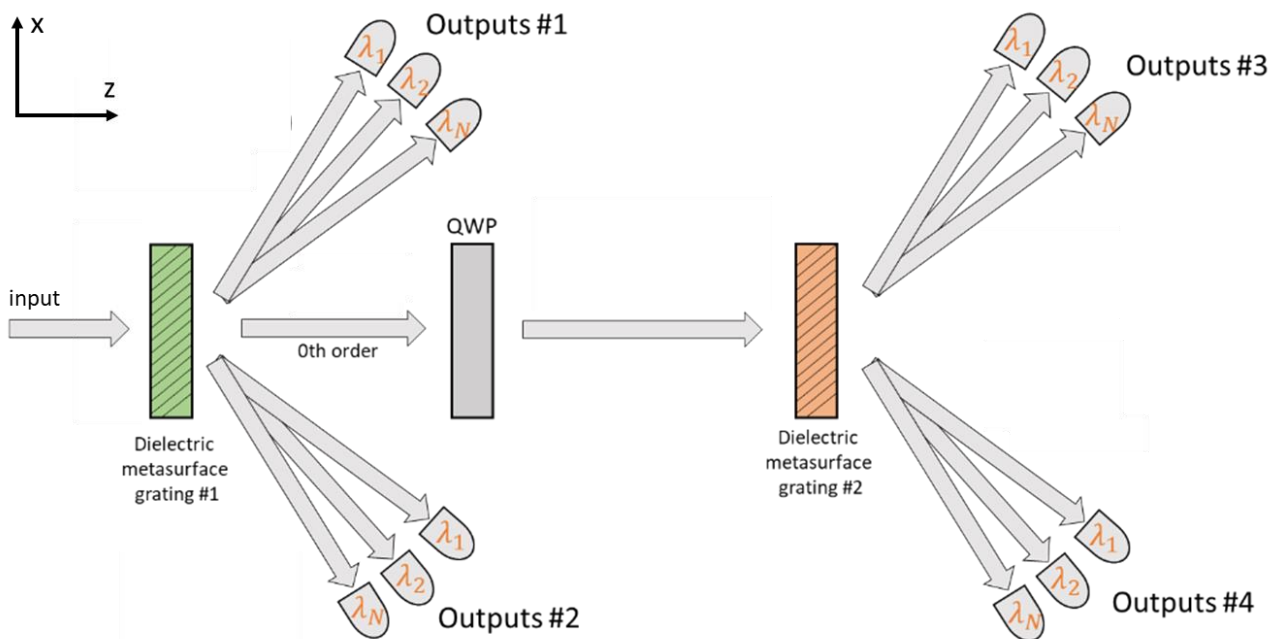


Figure 3. Compact scheme for polarization state analysis utilizing two Berry-phase metasurfaces (green and red element) with a quarter-wave-plate in between. The decomposition is performed into linear and circular polarization.

The approach takes advantage of two Berry phase meta-surfaces. Both surfaces implement a linear phase with the rotation angle  $\phi(x,y) = \pi * x / P$  being a function of x coordinate only (see also Figure 1). P denotes the spatial extension (the period) after which the rotation of the basic meta-atom (pillar) achieves 180°, such that the generated structure is identically replicated. Thinking in terms of diffractive optics (and neglecting for a moment QKD and the special polarization response of a Berry phase element) then both metasurfaces implement nothing else then a *blazed grating* diffracting light into its first diffraction orders. As usual, the diffraction angle depends on the wavelength according to  $\sin(\alpha) = \pm\lambda/P$ . However, thanks to the nature of the Berry phase metasurface the diffraction efficiency depends on the polarization of the incident light and thus left-handed and right-handed circular polarization is routed into opposite direction.

Up to now, we only have outlined the spatial arrangement of both meta-surfaces (which is identical), but we did not refer to the particular functionality or characteristics of the single meta-atom itself. Looking to Figure 3, it is obvious that the meta-atoms of both elements (green vs. orange) must be different since the first meta-surface (green) offers a non-zero probability to forward a photon along the optical axis (z-axis) whereas the second meta-surface (orange) does not. Referring to Section 2 and in particular to Table 1 will answer this question. The first Berry phase element (green) is composed of meta-atoms which act as quarter-wave-retarders (QWR) whereas the second element (orange) is composed of different meta-atoms acting as half-wave-retarders (HWR). Combining the results outlined in Table 1 and taking into account the sequential arrangement as depicted in Figure 3 (with the quarter wave plate in between), then the following polarization analysis scheme can be deduced:

Table 2. Ideal probability that a polarized single photon is detected in one of the four main detection channels of the optical configuration as depicted in Figure 3.

$j_{IN}$	Output #1	Output #2	Output #3	Output #4
$ 0\rangle$	25%	25%	0%	50%
$ 90\rangle$	25%	25%	50%	0%
$ LHC\rangle$	50%	0%	25%	25%
$ RHC\rangle$	0%	50%	25%	25%

## 5. MODELLING RESULTS

The previous sections were rather dominated introducing and discussing theoretical concepts and their ideal performance. In consequence, we will now focus on expected real-world performances and as such we will present modelling results of specific Berry phase elements which are suited to be utilized in the new polarization analysis scheme introduced in Section 4.

As an example, we will present the design of the optical nanostructures (pillars) tailored for operation within the ITU grid between wavelengths of 1530nm and 1570nm. As already mentioned in Section 2, silicon (pillars) on glass (substrate) is the material system of choice when working in the infrared spectrum. Most notably, the patterning of silicon nanostructures can be addressed by well-established lithographic technology workflows taking advantage of semi-conductor manufacturing processes.

**Single Pillar Optical Performance.** The fundamental geometrical layout of the single meta-atom (pillar) is exactly that already presented in Figure 1. Carefully adjusting the three cartesian extensions allows to find two suitable solutions where the single pillar offers either quarter-wave- or half-wave-retardation. Figure 4 shows the optical modeling results (transmission efficiency and phase) for a periodically replicated uniform pattern of pillars. The left part presents the performance of the QWR and the right part that of the HWR. The insets provide a top view sketch of the corresponding structures and they clearly emphasize, that the precise dimensions are different although the pitch (distance between the centers of neighboring pillars) is equal, i.e. 600nm.

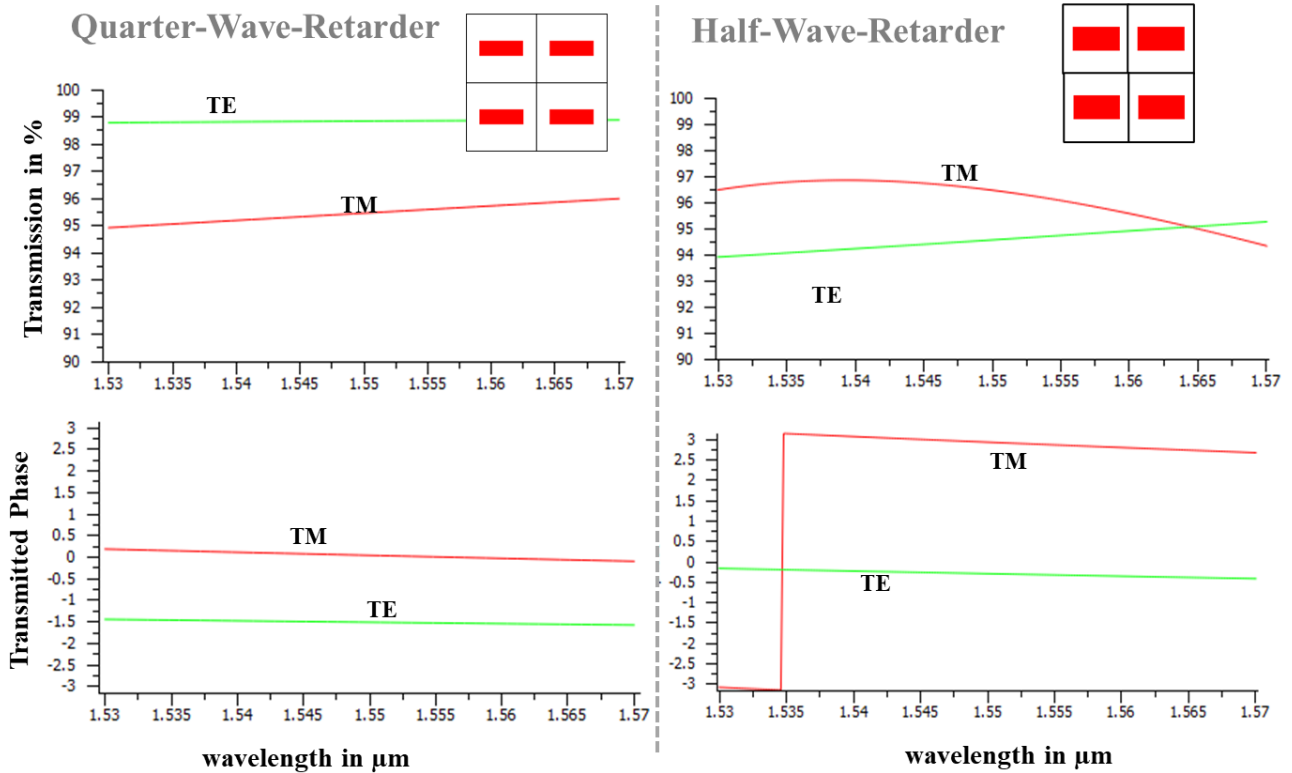


Figure 4. Efficiency and phase of the transmitted light of periodically arranged silicon pillars depending on the linear state of polarization. The direction of TE and TM polarization coincides with the long axis or the short axis of the pillars, respectively.

Both solutions show very good transmission efficiencies above 95% and the phase retardation is either  $\pi/2$  or  $\pi$ , respectively. The missing amount of light goes dominantly into reflection and can be considered as Fresnel-reflection losses which are typical for any kind of optical interface where the refractive index of the underlying material is different.

**Berry Phase Element.** In order to realize the metasurface elements needed to built up the polarization analysis configuration as outlined in Section 4, the single pillars must be arranged in a rotated fashion in order to create Berry phase elements acting as polarization sensitive *blazed meta-gratings*. Furthermore, it is desired to minimize the period of the meta-gratings as much as possible. This helps to maximize the diffraction angle of the first diffraction orders (corresponding to the outputs #1 to #4, see Figure 3) and thus allowing to design the overall setup as compact as possible.

The following figures present the modelled optical performance of both meta-gratings, the first being composed of QWR pillars and the second being composed of HWR pillars. Please note that the following discussion will mainly refer to diffraction efficiencies, however, in QKD applications they must be interpreted as routing probabilities of single photons.

The insets of Figure 5 and Figure 6 show a sketch of each meta-grating's actual nanostructure. In either case, the pitch between neighboring elements is 600nm, the unit cell of the grating is composed of 6 rotated pillars with a difference in rotation angle of  $180^\circ / 6 = 30^\circ$  between consecutive elements. Focusing on some representative scenarios, it can be seen that the meta-grating being composed of HWR elements diffracts nearly 94% of circularly polarized input beam into the +1<sup>st</sup> diffraction order (later corresponding to output #3 of the overall device). Moreover, the efficiency dispersion is very weak throughout the entire bandwidth. At the same time a very low fraction  $<1\%$  is routed into the 0<sup>th</sup> or higher diffraction orders such that it is lost for analysis purposes. On the contrary, the amount of light which is routed into the opposite -1<sup>st</sup> diffraction order (later corresponding to output #4 of the overall device) is only  $<10^{-4}$ , corresponding to a contrast of  $>10000$ . This characteristics is very important since it determines the residual cross-coupling probability between different outputs of the

envisaged polarization analysis configuration. Lower contrasts will increase the error rate for QKD applications accordingly.

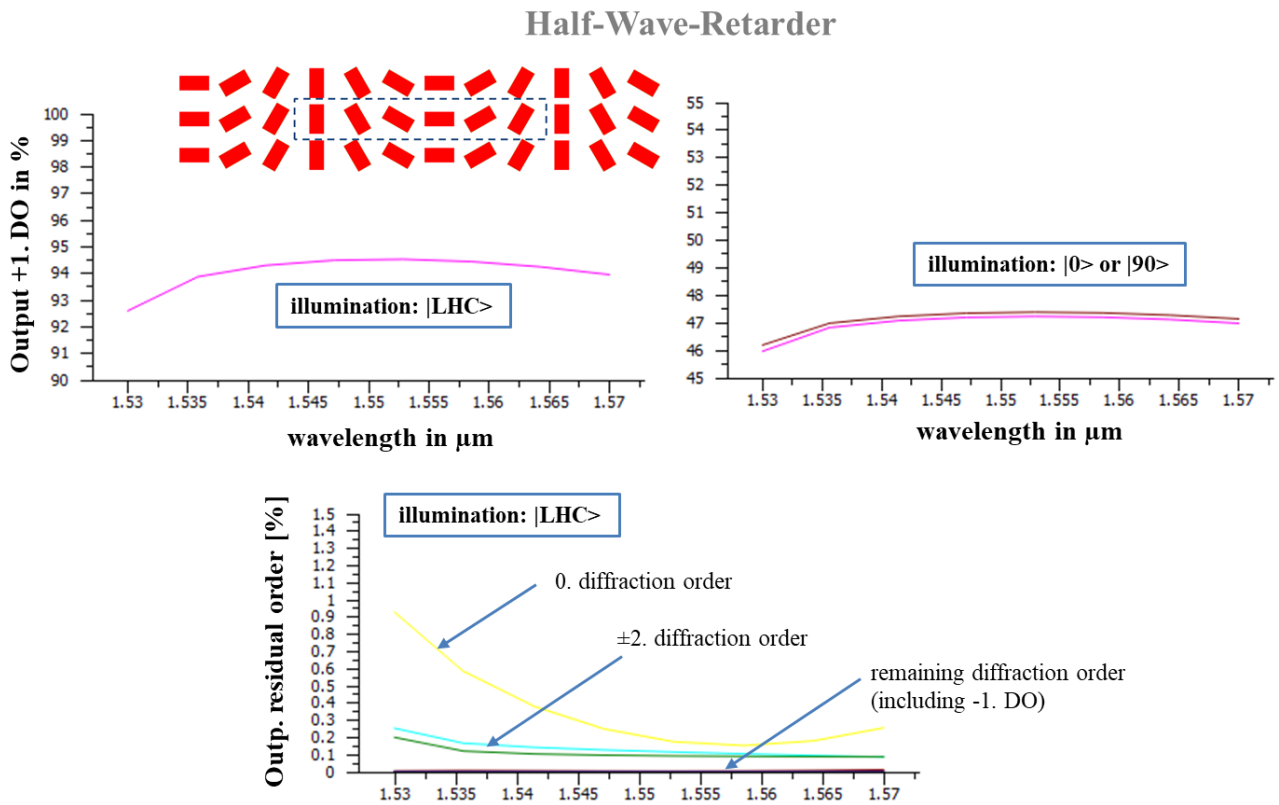


Figure 5. Selected probabilities for routing a polarized photon into different diffraction orders of the Berry phase meta-grating composed of HWR-pillars.

The meta-grating being composed of QWR elements is considered in Figure 6. Considering circularly polarized incident light (left part), then the splitting between +1<sup>st</sup> and 0<sup>th</sup> diffraction order is well-balanced, nevertheless, the efficiency dispersion is larger than those for the HWR-meta-grating. Although not explicitly shown, the cross-coupling contrast between +1<sup>st</sup> and -1<sup>st</sup> order is larger than 1000, meaning that a photon with e.g. left-handed circular polarization is routed into the opposite (wrong) channel with a probability  $<10^{-3}$ . The overall efficiency (the sum of 0<sup>th</sup> order and  $\pm 1$ <sup>st</sup> order) is well comparable with that of the previous element, i.e.  $\sim 95\%$ .

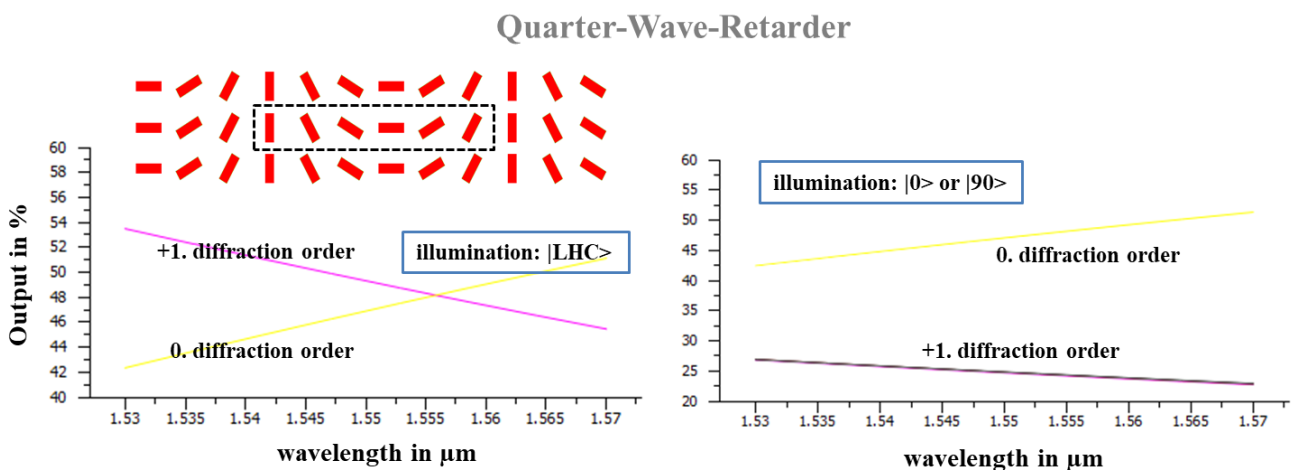


Figure 6. Selected probabilities for routing a polarized photon into different diffraction orders of the Berry phase meta-grating composed of QWR-pillars.



## 6. CONCLUSION

We have presented a new and compact configuration for optical polarization state analysis which we think is particularly advantageous in QKD free space application with large apertures. It relies on the utilization of two Berry phase meta-gratings, a special class of dielectric metasurfaces which allows to tailor the optical response depending on the polarization of the incident light or photon. First, we have outlined the theoretical performance limits. In addition, we have presented modelling results of a particular realization using silicon on glass metastructures designed to operate in the telecommunication band around 1550nm. The overall efficiency of each component is in the order of 95%. However, the cross-coupling contrast between different channels of the polarization analysis setup is verified to be larger than  $10^3$  or even  $10^4$ , respectively. The overall approach is well suited to be scaled to other spectral bands which might be used for optical free space communication, e.g. around 1064nm or 850nm. Silicon on glass metastructures might be feasible for wavelengths around 1064nm, however, at wavelengths at 850nm the material system most likely has to be adapted, e.g. to titanium dioxide on glass.

## 7. ACKNOWLEDGEMENTS

The authors acknowledge the funding of this work by the German Ministry of Education and Research (BMBF) in project *QuNet Beta* under grant number XXYYZZ.

## 8. REFERENCES

- [1] Bennett C.H. and Brassard G., *Quantum cryptography: Public key distribution and coin tossing*, Theoretical Computer Science, Vol. 560, 7-11, 2014
- [2] Ekert A.K., *Quantum cryptography based on Bell's theorem*, Phys. Rev. Lett., Vol. 67, 661-663, 1991
- [3] Chen W.T., Zhu A.Y. and Capasso F., *Flat optics with dispersion-engineered Metasurfaces*, Nature Reviews Materials, Vol. 5, 604-620, 2020
- [4] Jung J., Park H., Park J., Chang T. and Shin J., *Broadband metamaterials and metasurfaces: a review from the perspectives of materials and devices*, Nanophotonics, Vol. 9(10), 3165–3196, 2020
- [5] Huang L., et al., *Dispersionless Phase Discontinuities for Controlling Light Propagation*, Nano Letters, Vol. 12, 5750–5755, 2012
- [6] Chen X., et al., *Dual-polarity plasmonic metalens for visible light*, Nature Comm., Vol. 3, 1198, 2012
- [7] Zheng S., et al., *Experimental realization to efficiently sort vector beams by polarization topological charge via Pancharatnam–Berry phase modulation*, Photonics Research, Vol. 6(5), 385–389, 2018